JOURNAL OF CIVIL ENGINEERING AND MANAGEMENT
ISSN 1392-3730 print/ISSN 1822-3605 online
2012 Volume 18(1): 60–70
doi.org/10.3846/13923730.2011.652982

ACOUSTICALLY ASSESSED INFLUENCE OF AIR PORE STRUCTURE ON FAILURE OF SELF-COMPACTING CONCRETES UNDER COMPRESSION

Tomasz Gorzelańczyk

Institute of Building Engineering, Wrocław University of Technology,
Wybrzeże Wyspiańskiego 27, 50-370 Wrocław, Poland
E-mail: tomasz.gorzelanczyk@pwr.wroc.pl

Received 29 May 2011; accepted 06 Oct. 2011

Abstract. The paper presents the results of investigations into the influence of pore structure on the failure of self-compacting concretes modified with superplasticizers commonly used in construction. Pore structure examinations were carried out in practically the whole range of pore diameters by means of an image analyzer and a mercury porosimeter. The failure of the self-compacting concretes under compression, was investigated by the acoustic emission technique and other methods. The levels of cracking initiating stress σ_i and critical stress σ_{cr}, demarcating the different stages in the failure process, were determined. It has been shown that there is a relationship between the pore structure parameters and the levels. The fatigue strength of the self-compacting concretes was calculated from the experimental results and on this basis the suitability of the concretes for structures subject to cyclic loads was determined.

Keywords: self-compacting concrete, pore structure, failure, compression, acoustic emission, ultrasounds.

1. Introduction

Self-compacting concretes are increasingly often used to erect buildings and civil engineering structures (Klug, Holschemacher 2003; Holschemacher 2004; Okamura, Ouchi 1999, 2003; Okamura *et al.* 2005). Concrete mixes used for this purpose are modified with superplasticizers based on different chemical components and producing a similar rheological effect. But the question arises: does the air pore structure in hardened self-compacting concretes depend on the added superplasticizer? If so, does this structure affect the failure of the concrete? The answers to these questions can be useful in, for example, predicting the performance of self-compacting concrete in service. This applies particularly to concrete built into structures subject to cyclic loads, such as bridge deck slabs, industrial floors and concrete road surfaces. Therefore it seems interesting and desirable to examine the failure of such concretes and determine the levels of cracking initiating stress σ_i and critical stress σ_{cr}, demarcating the different stages in this process. It is generally accepted that these properties have a bearing on the durability of concrete (Błaszczyński 2011; Furtak 2002; Hoła 2002; Kmiecik, Kamiński 2011; Sadowski 2010; Trapko, Musiał 2011). The failure of ordinary concretes, high-performance concretes and concretes saturated with methyl methacrylate is described in the literature (Broniewski *et al.* 1994; Furtak 2002; Hoła 1992, 2000b; Newman, K., Newman, J. B. 1971; Ngab *et al.* 1981), but little is known about the course of this process in self-compacting concretes.

Considering the above, the air pore structure of several self-compacting concretes made with additions of two most commonly used superplasticizers was examined. Then the failure of the concretes was investigated using acoustic techniques and the levels of cracking initiating stress σ_i and critical stress σ_{cr}, demarcating the different stages in this process, were determined. The results were used to calculate the fatigue strength of the concretes. On this basis the authors drew a conclusion about the suitability of the concretes for structures subject to cyclic loads. It should be mentioned that the proof that the fatigue strength of concrete depends on the levels of cracking initiating stress σ_i and critical stress σ_{cr} can be found in the literature (Beres 1971; Flaga 1995; Furtak 1997; Hsu 1981).

2. Investigations

Four self-compacting concretes, denoted as: A/S_A, B/S_A, C/S_V and D/S_V, made of the same components, i.e. Portland cement CEM I 42.5 R, gravel aggregate, river sand, fly ash (chemical composition of the fly ash: SiO_2 51%, Al_2O_3 24%, Fe_2O_3 6.8%, CaO 0.3%, $S0_3$ 0.5%; power plant based on hard coal), drinking tap water and two different superplasticizers were subjected to tests. The maximum aggregate grading was 16 mm for concretes A/S_A and C/S_V and 8 mm for concretes B/S_A and D/S_V. Superplasticizer S_A was added to make concretes A/S_A and B/S_A while concretes C/S_V and D/S_V were made using superplasticizer S_V. Superplasticizer S_A was based on polycarboxylic ether while superplasticizer S_V was based

Table 1. Compositions of designed self-compacting concrete mixes and average compressive strengths f_{cm} of concretes produced from them

Mix and concrete symbol	Concrete mix composition [kg/m^3]						Water-binder ratio $\frac{W}{C+P}$	Sand content [%]	Average compressive strength f_{cm} after 90 days of curing [MPa]
	Coarse aggregate	Sand	Cement	Fly ash	Water	Super-plasticizer			
A/S_A	1064	581	355	143	164	3.15	0.34	35.3	44.5 4.2%*)
B/S_A	896	747	325	109	195	3.25	0.45	45.5	32.4 4.8%*)
C/S_V	1064	581	355	143	164	4.18	0.34	35.3	59.2 5.1%*)
D/S_V	896	747	325	109	195	4.25	0.45	45.5	41.8 5.8%*)

*) Note: the variation coefficient value

Table 2. Determined rheological properties of concrete mixes

Test method	Tested parameter	Requirements acc. to Li and Hwang (2003), Nagamoto and Ozawa (1999), Okamura and Ouchi (2003), European Project Group (2005)	Test results			
			Concrete mix symbol			
			A/S_A	B/S_A	C/S_V	D/S_V
Abrams cone	500 mm diameter spread time T_{500} [s]	2–5	5.0	4.6	4.9	4.1
	Spread diameter r [mm]	650–800	680	660	690	710
J-Ring	Difference between measured spread diameters $\lvert d_1 - d_2 \rvert$ [mm]	≤ 50	30	25	35	30
L-Box	Ratio of measured heights H_2/H_1 [–]	0.80–1.00	0.87	0.85	0.92	0.93

on a combination of polycarboxylates and viscosity, setting and hardening regulators. The two superplasticizers are used in construction practice to make self-compacting concrete mixes.

The compositions of the designed concrete mixes are shown in Table 1. The latter also includes average compressive strengths f_{cm} of the concretes produced from the mixes, determined on 150×150×150 mm samples after 90 days of curing in a climate chamber at an air temperature of +18 °C (±1 °C) and a relative air humidity of 95% (±5%).

The concrete mixes were tested to determine their basic rheological properties, using the Abrams cone, the J-Ring method and the L-Box method. The results of the tests are shown in Table 2. Fig. 1 shows exemplary J-Ring spread test results for mix A/S_A (Fig. 1a) and L-Box flow tests results for mix D/S_V (Fig. 1b). The tests confirmed that the rheological properties of the designed concrete mixes met the requirements for self-compacting mixes (Li, Hwang 2003; Nagamoto, Ozawa 1999; Okamura, Ouchi 2003; European Project Group 2005). It also became apparent that despite the fact that they differed in their superplasticizers and maximum aggregate grading (16 and 8 mm), the mixes were characterized by very similar rheological properties.

The air pore structure in the four hardened 90-day old concretes was examined in a diameter range of 10–4000 μm by means of a computer image analyzer Image Pro Plus 4.1 (Fig. 2a) and in a radius range of 5–7500 nm by means of a mercury porosimeter Carlo Erba Strumentazione model 2000 (Fig. 2b). In the former case the determined air pore structure parameters were: total air content (A), below-0.3 mm-diameter micropore content (A_{300}), air pore distribution index ($\overline{L}$) and air pore specific surface area (α). In the latter case the following parameters were determined: total porosity (p), specific pore volume (V), average pore radius ($\overline{r}$) and specific pore area (α').

The failure process was investigated using an Instron 1126 strength tester and two acoustic techniques (Hoła, Schabowicz 2010), i.e. the ultrasonic technique and the acoustic emission technique. 100×100×100 mm concrete samples were used in the ultrasonic investigations. Longitudinal ultrasonic wave velocity V_L was the investigated parameter, determined (perpendicularly to the direction of load action) as a function of compressive strength. An UNIPAN 543 ultrasonic probe with digital readout, and 100 kHz ultrasonic heads were used in the investigations. 50×50×100 mm samples (cut out from larger test pieces) were used in the acoustic emission investigations. As they were being compressed, the following AE descriptors were recorded: rate of events N_{zd} and *RMS* signal. Friction at the contact between the specimen's surface and the strength tester's pressure plates was eliminated by grinding the surfaces to ensure their mutual parallelism with accuracy to 0.05 mm and then greasing them. A Vallen-Systeme Gmbh AMS3 measuring set and two VS 150-M sensors with a transmission band of 100–450 kHz were used in the investigations. Fig. 3 shows the AE measurement rig.

a) b)

Fig. 1. Spread test results for: a) concrete mix A/SA (J-Ring); b) concrete mix D/SV (L-Box)

a) b)

Fig. 2. Rigs for investigating air surface pores in hardened concrete by means of: a) image analyzer; b) mercury porosimeter

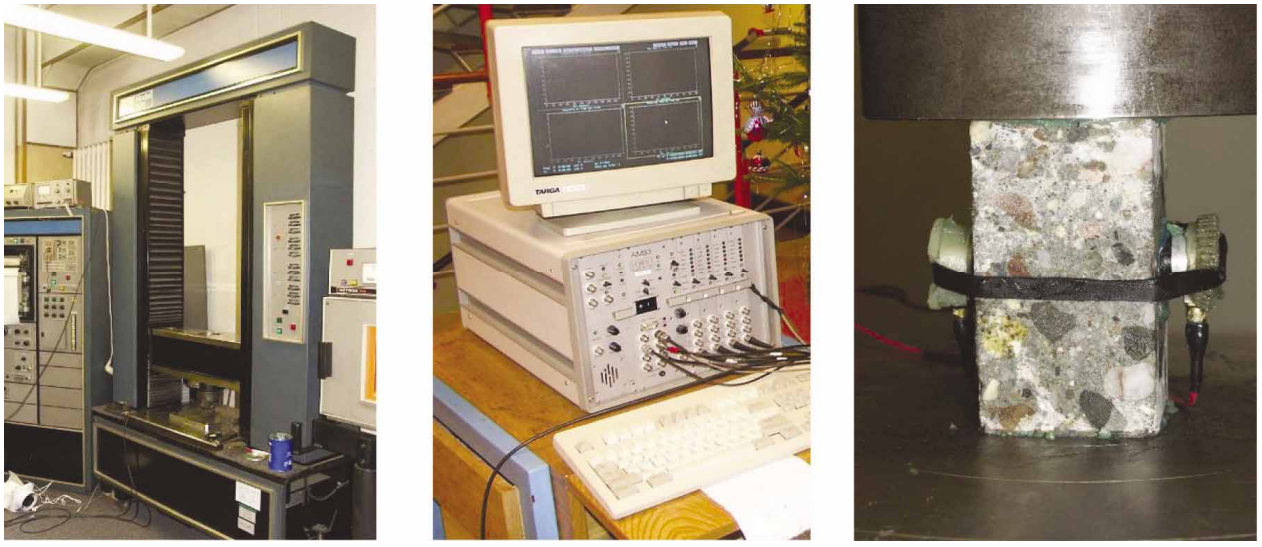

a) b) c)

Fig. 3. Rig for measuring acoustic emission in compressed concrete: a) strength tester Instron 1126; b) measuring set Vallen-Systeme Gmbh AMS3; c) concrete specimen prepared for testing

Table 3. Averaged values of selected parameters characterizing pore structure of compared concretes A/S_A and C/S_V and B/S_A and D/S_V

Investigated parameter	Concrete batch symbol			
	A/S_A	B/S_A	C/S_V	D/S_V
Total air content in hardened concrete A [%]	6.70	8.30	2.90	4.45
Below-0.3 mm-diameter pore content A_{300} [%]	1.50	2.96	0.70	1.74
Air pore distribution index $\overline{L}$ [mm]	0.26	0.11	0.33	0.13
Specific air pore surface area α [mm^{-1}]	17	36	21	45
Total porosity p [%]	12.71	13.02	11.90	12.44
Specific pore volume V [mm^3/g]	24.08	32.81	17.85	29.35
Average pore radius $\overline{r}$ [nm]	3.90	6.20	6.15	15.70
Specific pore surface area α' [m^2/g]	7.12	3.97	2.66	2.88

3. Results of porosity structure investigations

The results of the porosity structure investigations for the hardened 90 day-old self-compacting concretes (A/S_A and B/S_A and C/S_V and D/S_V) are shown in Table 3. Diagrams illustrating the results are shown in Figs 4–6.

According to Table 3, total air content A, below-0.3 mm-diameter pore content A_{300}, total porosity p, specific pore volume V and specific pore surface area α in concrete C/S_V modified with superplasticizer S_V are substantially lower than in concrete A/S_A modified with superplasticizer S_A. Whereas pore distribution index $\overline{L}$, average pore radius $\overline{r}$ and specific air pore surface α are higher for concrete C/S_V. Therefore one can conclude that the polycarboxylic ether in superplasticizer S_A causes considerable air entrainment in the self-compacting concrete. A similar conclusion emerges from the investigations carried out by the authors Gorzelańczyk and Hoła (2007), Khatib and Mangat (1999), Łaźniewska-Piekarczyk (2009), Szwa-bowski and Łaźniewska (2007).

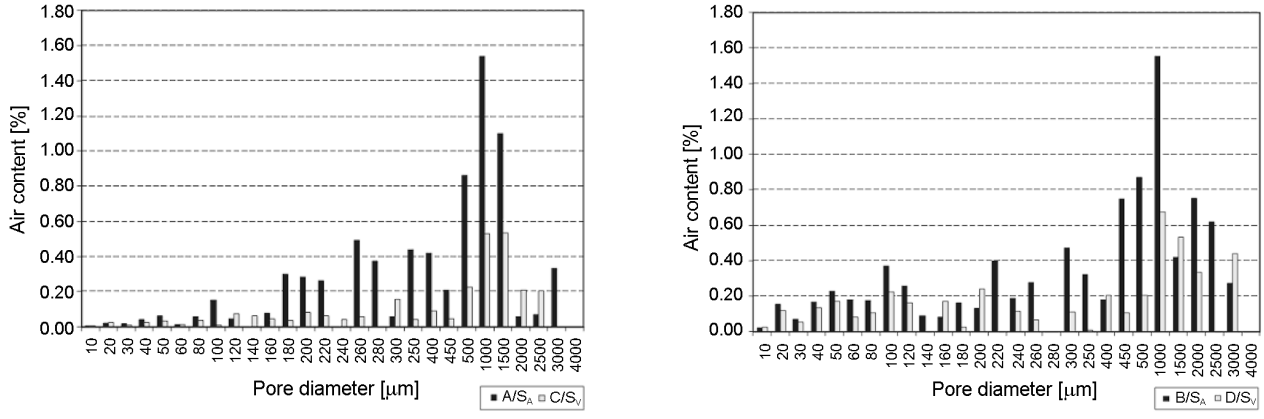

Fig. 4. Air pore content distribution depending on pore diameter in concretes: a) A/S_A and C/S_V; b) B/S_A and D/S_V

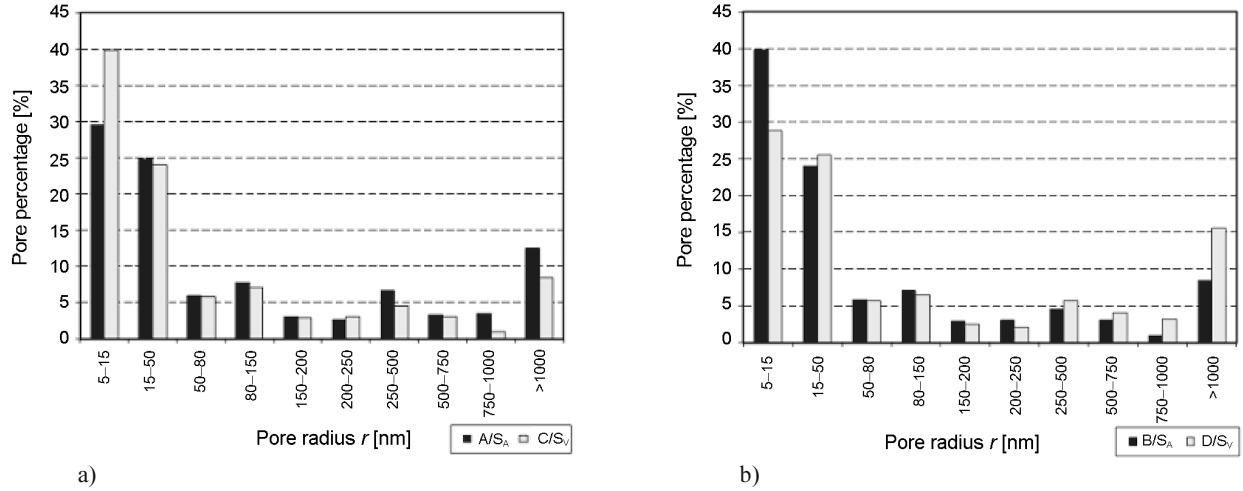

Fig. 5. Pore percentage for adopted radius intervals in pore radius range of 5–7500 nm for compared concretes: a) A/S_A and C/S_V; b) B/S_A and D/S_V

According to Fig. 4a, the air content in concrete C/S_V is lower almost in the whole test range of pore diameters. This is particularly visible in a pore diameter range of 180–1500 μm. A similar conclusion emerges from Fig. 6, with the difference that in the whole range of pore radii the porosity of concrete C/S_V is lower than thatof concrete A/S_A. This means that the air pore structure in concrete C/S_V modified with superplasticizer S_V is characterized by better parameters than that of concrete A/S_A. Similar conclusions regarding concretes B/S_A and D/S_V emerge from Table 3 and Fig. 4b, i.e. concrete D/S_V, modified with superplasticizer S_V, has better air pore structure parameters.

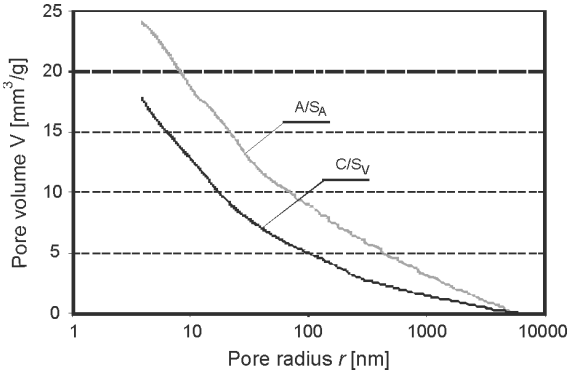

Fig. 6. Porosity characteristics of compared concretes A/S_A and C/S_V in pore range of 5–7500 nm (pore volume V versus pore radius r)

Fig. 5 shows that the percentage of pores whose radius is in a range of 5–7500 nm is lower in concrete C/S_V than in concrete A/S_A. Practically, only in a pore radius range of 5–15 nm concrete C/S_V has a higher pore percentage. In concrete D/S_V this is true only in a pore radius range 50–500 nm.

The above analysis of the porosity structure investigation results shows clearly that the air pore structure differs between the self-compacting concretes. It depends on the superplasticizer used to modify the concrete mix. It also appears that the air pore structure in concrete C/S_V modified with superplasticizer S_V, as compared with concrete A/S_A, and in concrete D/S_V modified with superplasticizer S_V, in comparison with concrete B/S_A, is characterized by better parameters.

4. Failure investigation results and their analysis

The failure investigation results of the self-compacting concretes, obtained by the acoustic techniques, are compared for concretes A/S_A and C/S_V and concretes B/S_A and D/S_V in Figs 7–11.

Fig. 7 shows curves of longitudinal ultrasonic wave velocity versus relative compressive strength in concretes A/S_A and C/S_V (Fig. 7a) and in concretes B/S_A and D/S_V (Fig. 7b), with marked levels of initiating stress σ_i and critical stress σ_{cr}, determined using the criteria given in Gorzelańczyk (2007, 2011) and Hoła (2000b). As already mentioned, the levels demarcate the stages of failure of concrete under compression (Furtak 2002; Hoła 1994, 2000a; Newman K., Newman J. B. 1971; Ngab *et al.* 1981) and are the visual effect of this process, observed during laboratory tests.

The results presented in Fig. 7 show that longitudinal ultrasonic wave velocity V_L in the concretes decreases as the compressive stress level increases. Similarly as in ordinary and high-performance concretes (Hoła 2000a; K. Newman, J. B. Newman 1971), the velocity begins to fall at a certain stress level, falling ever faster when the latter is exceeded. The stress level is not the same in all the tested concretes. Velocity V_L begins to fall at 0.33 σ_c/f_c and 0.38 σ_c/f_c. in respectively concrete A/S_A and C/S_V. The velocity of longitudinal ultrasonic waves in the concretes can be measured only up to a certain stress level since they are completely dampened when the latter is exceeded. The stress level is 0.90 σ_c/f_c and 0.93 σ_c/f_c in respectively concrete A/S_A and C/S_V. The levels are marked in Fig. 7a.

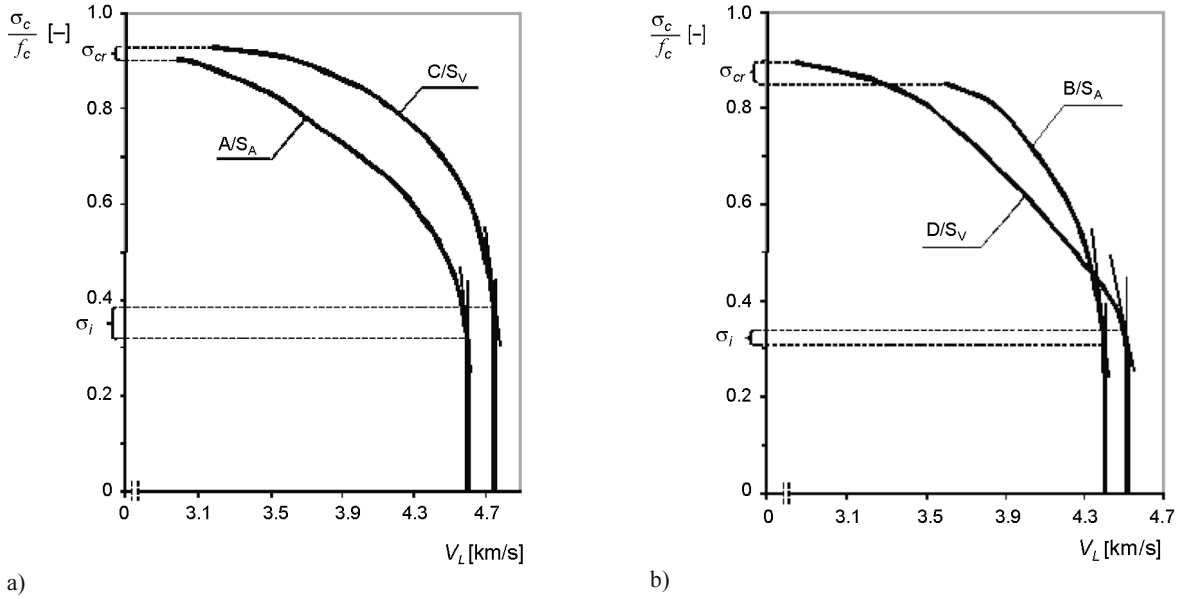

Fig. 7. Longitudinal ultrasonic wave velocity versus relative compressive stress in concretes: a) A/S_A and C/S_V; b) B/S_A and D/S_V

The investigations showed that the levels of cracking initiating stress σ_i and critical stress σ_{cr} are higher in concrete C/S_V, made using superplasticizer S_V, than in concrete A/S_A made using superplasticizer S_A. The same was found for concretes B/S_A and D/S_V, made using aggregate with the maximum grading of 8 mm (Fig. 7b).

Figs 8 and 9 show AE event rate N_{ev} over compression time for the compared concretes A/S_A and C/S_V and B/S_A and D/S_V. The RMS AE signal over compression time for the concretes is shown in Figs 10 and 11. Figs 8–11 include a plot of relative compressive stress σ_c/f_c versus failure time t, and levels of σ_i and σ_{cr}, determined according to the criteria given in Gorzelańczyk (2007) and Hoła (2000b).

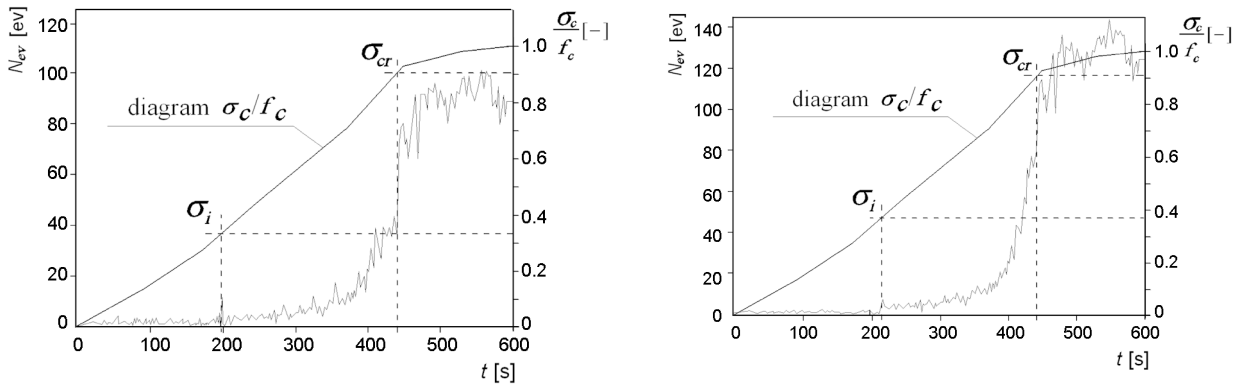

a) b)

Fig. 8. AE event rate N_{zd}, referred to relative compressive stress σ_c/f_c, versus failure time for self-compacting concrete: a) A/S_A; b) C/S_V

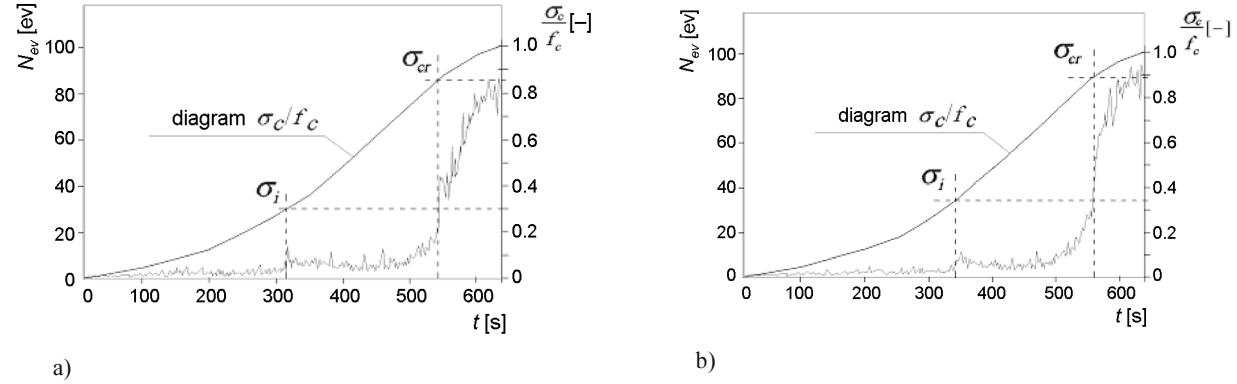

a) b)

Fig. 9. AE event rate Nzd, referred to relative compressive stress σ_c/f_c, versus failure time for self-compacting concrete: a) B/S_A; b) D/S_V

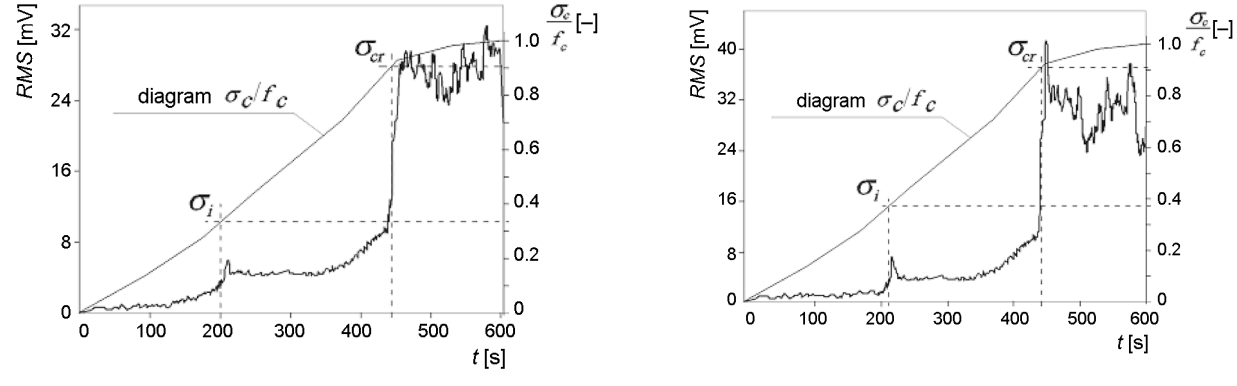

a) b)

Fig. 10. RMS AE signal, referred to relative compressive stress σ_c/f_c, versus failure time for self-compacting concrete: a) A/S_A; b) C/S_V

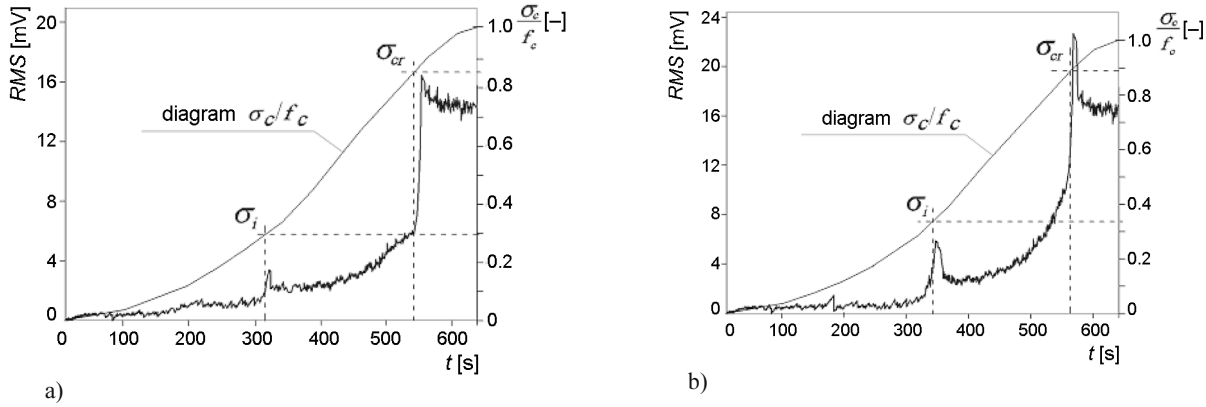

Fig. 11. RMS AE signal, referred to relative compressive strength σ_c/f_c, versus failure time for self-compacting concrete: a) B/S$_A$; b) D/S$_V$

According to Figs 8–11, the diagrams of event rate N_{ev} and the RMS AE signal versus failure time are similar for all the tested concretes: initially the values of the two recorded descriptors are small, then event rate N_{ev} and the RMS signal moderately increase and in the final stage of failure they sharply increase.

The results presented in Figs 7–11 clearly show that the failure of the ordinary and high-performance concretes proceeds in three stages.

The levels of cracking initiating stress σ_i and critical stress σ_{cr} in the compared concretes A/S$_A$ and C/S$_V$ and B/S$_A$ and D/S$_V$, determined in Figs 7–11, are compiled in Table 4. The table also includes (relative and absolute) average values of stresses σ_{im} and σ_{crm} calculated using the results obtained by means of the two investigative techniques.

It appears from Table 4 that in comparison with concrete A/S$_A$, concrete C/S$_V$ is characterized by a considerably higher level of cracking initiating stress σ_{im} and a slightly higher level of critical stress σ_{crm}. The same applies to concrete D/S$_V$ in comparison with concrete B/S$_A$. It should be noted that concretes C/S$_V$ and D/S$_V$ were made using superplasticizer S$_V$.

It should be noted here that as the literature survey (Gorzelańczyk 2007; Hoła 2002) indicates, cracking initiating stress in ordinary and high-strength concretes generally occurs a t a relatively higher relative compressive stress σ_c/f_c than in the self-compacting concretes tested here. This is due to, among other things, the composition of the self-compacting concretes: the latter contain much more fine-grain aggregate fractions and dusty additives than ordinary and high-strength concretes (Hoła 1992).

In order to illustrate the influence of air pore structure on the failure of the self-compacting concretes, diagrams of the dependence of the average relative levels of cracking initiating stress σ_{im} and critical stress σ_{crm} on such air pore structure parameters as: total air content A (Fig. 12), total porosity p (Fig. 13), air pore distribution index $\bar{L}$ (Fig. 14) and specific air pore surface area α (Fig. 15) were drawn.

It follows from Figs 12 and 13 that in the compared concretes A/S$_A$ and C/S$_V$ and B/S$_A$ and D/S$_V$ lower air content A and lower total porosity p are connected with higher levels of cracking initiating stress σ_{im} and critical stress σ_{crm}. The explanation can be that the lower the air content in the hardened concrete and the lower the total porosity, the smaller the number of places in which the structure is weakened. This is reflected in the fact that the stage of stable development of microcracks begins at a higher strain during the failure of the concrete.

Figs 14 and 15 show that higher pore distribution index $\bar{L}$ and larger specific air pore surface area α are connected with higher values of stress σ_{im} and stress σ_{crm}. Therefore one can conclude that when air pores are

Table 4. Levels of stress σ_i and σ_{cr} and (relative and absolute) average values of σ_{im} and σ_{crm} stress levels in concretes A/S$_A$, C/S$_V$, B/S$_A$ and D/S$_V$, determined by ultrasonic technique and AE technique

Concrete batch symbol	Measuring technique				Average values			
	Ultrasonic		AE		σ_{im}		σ_{crm}	
	σ_i [–]	σ_{cr} [–]	σ_i [–]	σ_{cr} [–]	[–]	MPa	[–]	MPa
A/S$_A$	0.33 8.7%*	0.90 2.1%	0.33 5.4%	0.91 4.2%	0.330	14.83	0.905	40.51
B/S$_A$	0.31 7.6%	0.85 1.5%	0.30 8.6%	0.86 7.5%	0.305	9.72	0.855	27.22
C/S$_V$	0.38 6.4%	0.93 2.1%	0.38 6.6%	0.92 4.4%	0.380	22.67	0.925	55.69
D/S$_V$	0.33 8.8%	0.90 1.3%	0.34 5.9%	0.90 2.9%	0.335	14.09	0.900	38.27

* Note: the variation coefficient value is given under the bar.

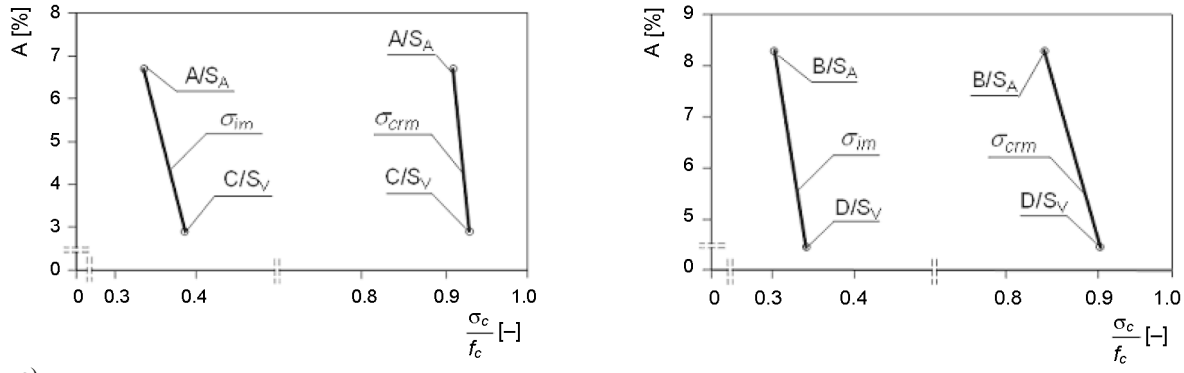

Fig. 12. Dependence of average relative levels of stress σ_{im} and σ_{crm} on total air content A in hardened self-compacting concrete (pore diameter range 10–4000 μm): a) A/S_A and C/S_V; b) B/S_A and D/S_V

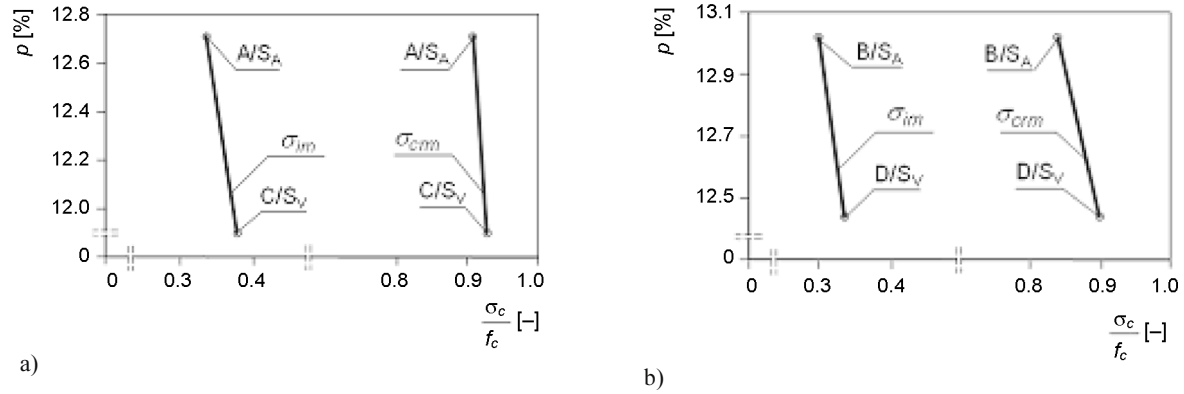

Fig. 13. Dependence of average relative levels of stress σ_{im} and σ_{crm} on total porosity p in hardened self-compacting concrete (pore radius range 5–7500 nm): a) A/S_A and C/S_V; b) B/S_A and D/S_V

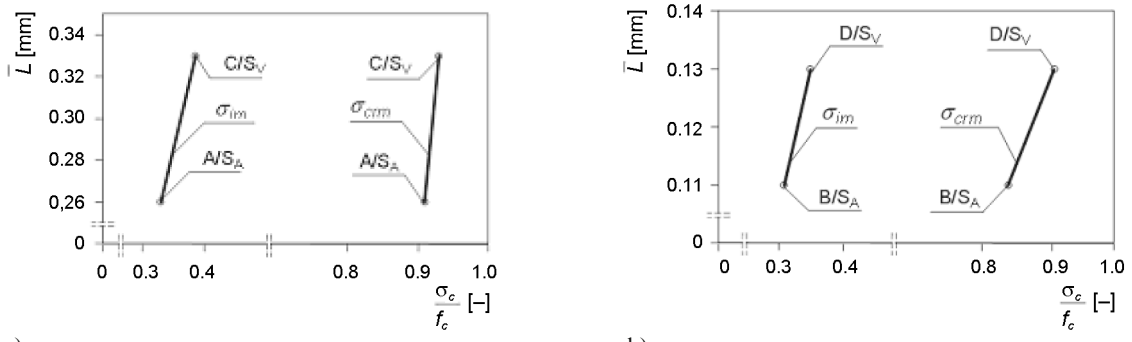

Fig. 14. Dependence of average relative levels of stress σ_{im} and σ_{crm} on air pore distribution index $\overline{L}$ in hardened self-compacting concrete (pore diameter range 10-4000 μm): a) A/S_A and C/S_V, b) B/S_A and D/S_V

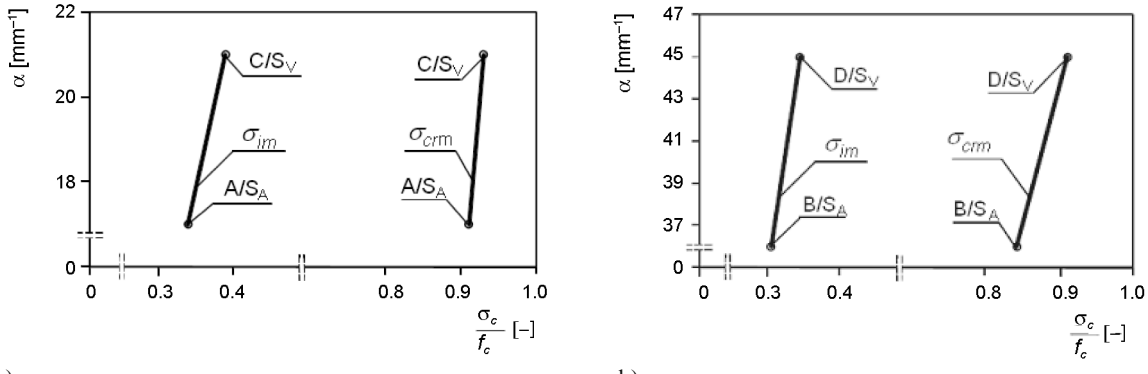

Fig. 15. Dependence of average relative levels of stress σ_{im} and σ_{crm} on specific air pore surface area α in hardened self-compacting concrete (pore diameter range 10–4000 μm): a) A/S_A and C/S_V; b) B/S_A and D/S_V

distributed more sparsely and their specific surface area is larger, then the structure is more homogenous. In such concrete the stage of stable propagation of cracks begins at a higher stress level and the stage of catastrophic failure is slightly shorter.

5. Using stress levels to calculate fatigue strength of concretes

The experimentally determined cracking initiating stress σ_i and critical stress σ_{cr} were used to calculate the fatigue strength of the concretes under compression from relation (1) given by Furtak (1997):

$$f_c^f / f_c = CN^{-A}\left(1 + B\rho^f \log N\right)C_f , \quad (1)$$

where: C – a coefficient expressing the ratio of dynamic strength to static strength under one-time loading (as in Furtak (1997)), the coefficient was assumed to be equal to 1.16); ρ^f – a stress ratio; $\sigma_c^{\min}$ – the minimum cycle stress; $\sigma_c^{\max}$ – the maximum cycle stress; C_f – a coefficient expressing the influence of load change rate on fatigue strength; A, B – coefficients representing the condition of concrete structure by being dependent on stress σ_i and σ_{cr}.

According to Furtak (1997), stress ratio ρ^f is described by the relation:

$$\rho^f = \sigma_c^{\min} / \sigma_c^{\max} , \quad (2)$$

and coefficient C_f can be described by the relation:

$$C_f = 1 + 0,07\left(1 - \rho^f\right)\log f , \quad (3)$$

where f is a load change rate [Hz] and coefficients A and B can be calculated from relations (4) and (5):

$$A = 0.008 - 0.118\log\left(\sigma_i / f_c\right), \quad (4)$$

$$B = 0.118\left(\sigma_{cr} / \sigma_i - 1\right). \quad (5)$$

Fig. 16 shows the fatigue strength of self-compacting concretes A/S_A, B/S_A, C/S_V and D/S_V versus number of stress cycles N, calculated using relation (1) and the average levels of stress σ_{im} and σ_{crm}. The calculations were done for stress ratio ρ^f = 0 and load change rate f = 1 Hz.

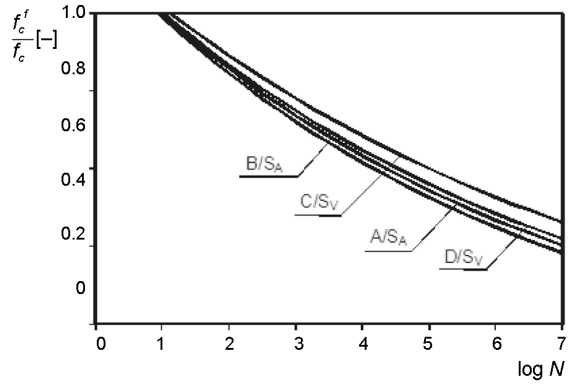

Fig. 16. Fatigue strength of concretes A/S_A, B/S_A, C/S_V and D/S_V versus stress cycles for ρ^f = 0 and f = 1 Hz

It appears from the Fig. 16 that concretes C/S_V and D/S_V modified with superplasticizer S_V have higher fatigue strength than concretes A/S_A and B/S_A modified with superplasticizer S_A.

6. Conclusions

1. There are significant differences in air pore structure between the four hardened self-compacting concretes made from the mixes characterized by similar rheological properties. The structure depends on the superplasticizer used in the making of the concrete mix. When superplasticizer S_V (based on a combination of polycarboxylates and viscosity, setting and hardening regulators) is added, the obtained structure is characterized by more advantageous parameters than the structure of the concrete made using superplasticizer S_A (based on polycarboxylic ether). The more advantageous parameters are:
   - lower total air content A;
   - lower below-0.3 mm-diameter micropore content A_{300};
   - lower total porosity p;
   - smaller specific pore volume V;
   - smaller specific pore area α';
   - higher pore distribution index $\overline{L}$;
   - larger specific pore surface area α;
   - larger average pore radius $\overline{r}$.

2. The investigations of the failure of the self-compacting concretes by means of the acoustic techniques (the ultrasonic technique and the acoustic emission technique) showed that air pore structure has an influence on the course of this process. The concretes made with the addition of superplasticizer S_V are characterized by higher levels of cracking initiating stress σ_i and critical stress σ_{cr} in comparison with the concretes made with the addition of superplasticizer S_A.

3. There are considerable differences in the fatigue strength calculated using the determined average levels of crack initiating stress σ_{im} and critical stress σ_{crm}, between the self-compacting concretes. The concretes made with the addition of superplasticizer S_V have higher strength than the concretes made with the addition of superplasticizer S_A. Therefore it can be stated that concrete mixes modified with superplasticizer S_V are more suitable for making structures which are subject to cyclic loads.

References

Beres, L. 1971. Fracture of concrete subjected to cyclic and sustained loading, *ACI Journal* 69(4): 304–305.

Błaszczyński, T. Z. 2011. Assessment of RC structures influenced by crude oil products, *Archives of Civil and Mechanical Engineering* 11(1): 5–17.

Broniewski, T.; Hoła, J.; Śliwiński, I. 1994. Application de la méthode d'émission acoustique aux essais du comportement du béton imprégné de polymère soumis á la compression [Application of the method of acoustic emission testing of the behavior of polymer impregnated concrete subjected to compression], *Materials and Structures* 27(170): 331–337.

European Project Group. 2005. *The European Guidelines for Self-Compacting Concrete: Specification, Production and Use* [cited 12 Apr. 2011]. Available from internet: <http://www.efnarc.org/pdf/sccguidelinesmay2005.pdf>.

Flaga, K. 1995. Wpływ naprężeń własnych na destrukcję naprężeniową i parametry wytrzymałościowe betonu [Effect of internal stresses on failure and strength parameters of concrete], *Inżynieria i Budownictwo* [Engineering and Construction] 6: 315–322.

Furtak, K. 1997. Wpływ wybranych czynników technologicznych na wytrzymałość zmęczeniową betonu, *Cement-Wapno-Beton* [Cement-Lime-Concrete] 4: 148–150.

Furtak, K. 2002. Destrukcja naprężeniowa betonu, in *"Days of Concrete – Tradition and Modernity*", Polski Cement, Szczyrk, 427–439.

Gorzelańczyk, T. 2007. *Ocena metodami akustycznymi procesu niszczenia betonów samozagęszczonych*. Reports of the Institute of Building Engineering at Wrocław University of Technology, PRE Ser., No. 9, Wrocław. 134 p.

Gorzelańczyk, T. 2011. The effect of moisture content on the failure of self-compacting concrete under compression, as assessed by means of acoustic methods, *Archives of Civil and Mechanical Engineering* 11(1): 45–60.

Gorzelańczyk, T.; Hoła, J. 2007. Assessment of the failure of self-compacting concretes differing in their air pore structure by acoustic techniques, in *Proc. of the 37th International Conference "Defektoskopie 2007"*, November, 2007, Prague, Czech Republic, 75–82.

Hoła, J. 1992. Effects of aggregate grading on the stress degradation of compressed concrete, *Archives of Civil Engineering* 38(1–2): 85–101.

Hoła, J. 1994. Emisja akustyczna w betonach [Acoustic emission in concretes], in I. Malecki and J. Ranachowski. *Emisja akustyczna. Źródła, metody, zastosowania*. Polska Akademia Nauk, Instytut Podstawowych Problemów Techniki, Warszawa, 223–240.

Hoła, J. 2000a. Determination of initiating and critical stress levels in compressed plain and high-strength concrete by acoustic methods, *Archives of Acoustics* 25(1): 57–65.

Hoła, J. 2000b. *Naprężenia inicjujące i krytyczne a destrukcja naprężeniowa w betonie ściskanym*. Scientific Papers of Institute of Building Engineering at Wrocław University of Technology, No. 76, Monograph Series No. 33, Wrocław University of Technology Publishing House, Wrocław. 182 p.

Hoła, J. 2002. Experimentally determined effects of technological and service factors on stress-induced destruction of concrete under compression, *Engineering Transactions* 50(4): 251–265.

Hoła, J.; Schabowicz, K. 2010. State-of-the-art non-destructive methods for diagnostic testing of building structures – anticipated development trends, *Archives of Civil and Mechanical Engineering* 10(3): 5–18.

Holschemacher, K. 2004. Hardened properties of self-compacting concrete, in Proc. of *the 8th International Conference "Modern building materials, structures and techniques"*, 19–21 May, 2004, Vilnius, Lithuania. Selected Papers, 55–60.

Hsu, T. C. T. 1981. Fatigue of plain concrete, *ACI Journal Proceedings* 78(4): 295–305.

Khatib, J. M.; Mangat, P. S. 1999. Influence of superplasticizer and curing on porosity and pore structure of cement paste, *Cement & Concrete Composites* 21(5–6): 431–437. doi:10.1016/S0958-9465(99)00031-1

Klug, Y.; Holschemacher, K. 2003. Comparison of the hardened properties of self compacting and normal vibrated concrete, in *Proc. of the 3rd RILEM Symposium on Self-Compacting Concrete*. Ed. by O. Wallevik and I. Nielsson, 2003, Reykjavik, Iceland, 596–605.

Kmiecik, P.; Kamiński, M. 2011. Modelling of reinforced concrete structures and composite structures with concrete strength degradation taken into consideration, *Archives of Civil and Mechanical Engineering* 11(3): 623–636.

Łaźniewska-Piekarczyk, B. 2009. The effect of superplasticizers and anti-foaming agents on the air entrainment and properties of the mix of self compacting concrete, *Cement-Wapno-Beton* [Cement-Lime-Concrete] 3: 133–147.

Li, L.-S.; Hwang, C.-L. 2003. The mixture proportion and property of SCC, in *Proc. of the 3rd RILEM Symposium on Self-Compacting Concrete*. Ed. by O. Wallevik and I. Nielsson, 2003, Reykjavik, Iceland, 525–529.

Nagamoto, N.; Ozawa, K. 1999. Mixture properties of Self-Compacting, High-Performance concrete, *ACI Materials Journal* 172: 623–636.

Newman, K.; Newman, J. B. 1971. Failure theories and design criteria for plain concrete, in M. Te'eni (Ed.). *Structure, Solid Mechanics, and Engineering Design*. London: Wiley-Interscience, 963–995.

Ngab, A. S.; Slate, F. O.; Nilson, A. H. 1981. Microcracking and time-dependent strain in high-strength concrete, *ACI Journal Proceedings* 78(4): 262–268.

Okamura, H.; Maekawa, K.; Mishima, T. 2005. Performance based design for self-compacting structural high-strength concrete, in *The 7th International Symposium on the Utilization of High Strength/High-Performance Concrete*, 20–24 June, 2005, Washington, USA, 13–34.

Okamura, H.; Ouchi, M. 1999. Self-Compacting Concrete: Development, present use and future, in *Proc. of the 1st RILEM Symposium on Self-Compacting Concrete*. Ed. by A. Skarendahl and O. Petersson, 1999, Stockholm, Sweden, 3–14.

Okamura, H.; Ouchi, M. 2003. Self-Compacting Concrete, *Journal of Advanced Concrete Technology* 1(1): 5–15. doi:10.3151/jact.1.5

Sadowski, Ł. 2010. New non-destructive method for linear polarisation resistance corrosion rate measurement, *Archives of Civil and Mechanical Engineering* 10(2): 109–116.

Szwabowski, J.; Łaźniewska, B. 2007. Influence of the properties of self-compacting concrete on the effect of air entrainment, in *The 9th International Conference "Modern Building Materials, Structures and Techniques"*, 16–18 May, 2007, Vilnius, Lithuania. Selected papers, 182–189.

Trapko, T.; Musiał, M. 2011. The effectiveness of CFRP materials strengthening of eccentrically compressed reinforced concrete columns, *Archives of Civil and Mechanical Engineering* 11(1): 249–262.

AKUSTIŠKAI ĮVERTINTA ORO PORŲ STRUKTŪROS ĮTAKA SUSITANKINANČIO BETONO SUSILPNĖJIMUI VEIKIANT GNIUŽDYMUI

T. Gorzelańczyk

Santrauka

Straipsnyje pateikiami porų struktūros įtakos susitankinančio betono su superplastikliais susilpnėjimui tyrimų rezultatai. Buvo atlikti praktiškai visų skersmenų porų struktūros tyrimai naudojant vaizdo analizatorių ir gyvsidabrio porosimetrą. Susitankinančio betono susilpnėjimas esant gniuždymui buvo tiriamas akustinės emisijos ir kitais metodais. Nustatyti pleišėjimo lygiai ir įtampos, žymintys skirtingus susilpnėjimo lygius. Parodyta, kad yra ryšys tarp porų struktūros parametrų ir susilpnėjimo lygių. Pagal eksperimentinius rezultatus suskaičiuotas betono atsparumas ir nustatytas betono tinkamumas konstrukcijoms, atsižvelgiant į ciklines apkrovas.

Reikšminiai žodžiai: susitankinantis betonas, porų struktūra, susilpnėjimas, gniuždymas, akustinė emisija, ultragarsai.

Tomasz GORZELAŃCZYK. PhD, Eng., researcher at Wrocław University of Technology, Poland. He obtained his diploma in civil engineering at the WUT in 2001. He is working at WUT, Institute of Building Engineering. Research interests: concrete (especially self-compacting concrete), failure of concrete, acoustic emission and other non-destructive tests.